Lowry, O. H., Rosenbrough, N. J., Farr, A. L., & Randall, R. J. (1951) *J. Biol. Chem. 193*, 265-275.
Maizel, J. V. C. (1971) *Methods Virol. 5*, 179-246.
Marinetti, G. V. (1962) *J. Lipid Res. 3*, 1-20.
Marsh, D., Watts, A., Pates, R. D., Uhl, R., Knowles, P. F., & Esmann, M. (1982) *Biophys. J. 37*, 265-271.
Privalov, P. L., & Khechinashvili, N. N. (1974) *J. Mol. Biol. 86*, 665-684.
Sedzik, J., Blaurock, A. E., & Hochli, M. (1984) *J. Mol. Biol. 174*, 385-409.
Sixl, F., Brophy, P. J., & Watts, A. (1984) *Biochemistry 23*, 2032-2039.
Stollery, J. G., Boggs, J. M., & Moscarello, M. A. (1984) *Biochemistry 19*, 1219-1226.
Suurkuusk, J., & Wadso, I. (1982) *Chem. Suipta 20*, 155-163.
Van Zoelen, E. J. J., Van Dijck, P. W. M., de Kruijff, B., Verkleij, A. J., & Van Deenen, L. L. M. (1978) *Biochim. Biophys. Acta 514*, 9-24.
Wiener, J. R., Wagner, R. R., & Freire, E. (1983) *Biochemistry 22*, 6117-6123.

An Electrical and Structural Characterization of H^+/OH^- Currents in Phospholipid Vesicles†

Walter R. Perkins and David S. Cafiso*
Department of Chemistry and Biophysics Program, University of Virginia, Charlottesville, Virginia 22901
Received August 26, 1985

ABSTRACT: Paramagnetic amphiphiles have been utilized to measure and characterize electrogenic H^+/OH^- ion transport in a series of model membrane systems. Membrane conductivity to H^+/OH^- ions varies with the method of vesicle preparation and with the level of saturation of the membrane phospholipid. Small sonicated vesicles have the lowest conductivities by approximately an order of magnitude compared to reverse-phase or ether-injection vesicle systems. This conductivity is particularly sensitive to the presence of polyunsaturated lipids in the vesicle membrane. The current-ΔpH dependence of the H^+/OH^- conductivity shows a nonideal behavior and renders the phenomenological membrane permeability dependent upon the experimental value of ΔpH that is chosen. These factors can account for much, if not all, of the variability in the published values for the H^+/OH^- permeability of model membranes. A procedure has been developed to establish and estimate changes in the dipole potential of vesicle bilayers. Using this method, we demonstrate that H^+/OH^- currents are insensitive to alterations in the membrane dipole field, a result that suggests that these currents are not rate limited by diffusion over simple electrostatic barriers in the membrane interior. In addition, conduction in D_2O has been examined, and we find that there is little difference in the magnitudes of D^+/OD^- currents compared to H^+/OH^- currents in vesicle systems.

Model membrane systems that are formed entirely of membrane phospholipids are generally exceedingly impermeable to small inorganic ions such as Na^+ and K^+. In small vesicles formed from egg phosphatidylcholine, these permeabilities typically range from 10^{-12} to 10^{-14} cm/s; as a consequence, gradients of these ions can be maintained for many weeks in these model membrane systems (Hauser et al., 1972; Johnson & Bangham, 1969; Pike et al., 1982; Mimms et al., 1981). Surprisingly, the apparent permeability determined for protons is many orders of magnitude larger than that for other monovalent ions. This observation has generated considerable interest, and a number of groups have reported both values and characteristics of this proton permeability [see, for example; Nichols et al. (1980), Nichols & Deamer (1980), Biegel & Gould (1981), Clement & Gould (1981), Nozaki & Tanford (1981), Gutknecht & Walter (1981), Rossignol et al. (1982), Deamer & Nichols (1983), Elamrani & Blume (1983), Cafiso & Hubbell (1983), Krishnamoorthy & Hinkle (1984), and Gutknecht (1984)]. These measurements have been carried out with a wide range of systems and techniques that are not necessarily directly comparable. While several features of this proton (or hydroxyl) flux are generally agreed upon (for example, the relative independence of the proton current on the size of the proton gradient, $[H^+]_{in} - [H^+]_{out}$), the values for the reported permeabilities vary by at least 4 orders of magnitude. The molecular basis for this conductivity is presently unknown.

In this paper, we have utilized a novel magnetic resonance approach, employing paramagnetic amphiphiles, to further characterize this net proton flux in a number of model membrane systems. The flux that we measure is electrogenic and is measured under conditions where no neutral flow of H^+/OH^- ions is detectable (Cafiso & Hubbell, 1983). The methodology we employ makes use of membrane-permeable phosphoniums, that we will refer to as I and II. These probes, which are easily monitored with EPR[1] spectroscopy, can be utilized to estimate H^+/OH^- ion currents in phospholipid vesicle systems. Using this methodology, we compare the proton permeability of both large and small unilamellar vesicles

† This research was supported by Grant J-61 from the Jeffress Trust, NSF Grant BNS 8302840, and a Camille and Henry Dreyfus Foundation grant for young faculty in chemistry (to D.S.C.).
* Author to whom correspondence should be addressed.

[1] Abbreviations: EPR, electron paramagnetic resonance; egg PC, egg phosphatidylcholine; POPC, 1-palmitoyl-2-oleoylphosphatidylcholine; OPPC, 1-oleoyl-2-palmitoylphosphatidylcholine; DOPC, dioleoylphosphatidylcholine; DAPC, diarachidonoylphosphatidylcholine; PAPC, 1-palmitoyl-2-arachidonoylphosphatidylcholine; DLPC, dilinoleoylphosphatidylcholine; SUV, sonicated unilamellar vesicle; LUV, large unilamellar vesicle; CCCP, carbonyl cyanide *m*-chlorophenylhydrazone; Ph_4B^-, tetraphenylboron anion; MES, 2-(*N*-morpholino)ethanesulfonic acid; MOPS, 3-(*N*-morpholino)propanesulfonic acid; tempoyl radical

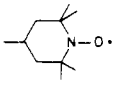

0006-2960/86/0425-2270$01.50/0

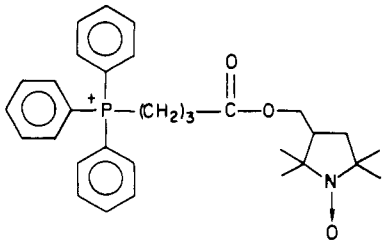

I

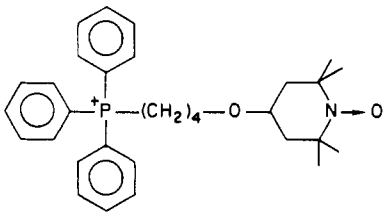

II

prepared by several techniques. We also examine the dependence of the protonic current upon the unsaturation of the membrane phospholipid and upon the experimental value of ΔpH that is chosen. Much, if not all, of the variability in the reported literature values can be accounted for by these experimental factors. We also describe a procedure for monitoring dipole potential changes in vesicles. This procedure is used to examine the dependence of the protonic current upon changes in the membrane dipole field (in an attempt to determine the percentage of charge flow due to positive vs. negative charge carriers). In addition, we compare the magnitudes of D^+/OD^- vs. H^+/OH^- currents in vesicle systems.

Materials and Methods

Spin-Labeled Probes. The phosphonium spin-label I and the secondary amine label *N*-tempoyl-*N*-hexylamine (III) were synthesized as previously described (Cafiso & Hubbell, 1978a,b). The spin-labeled phosphonium II was synthesized according to a procedure described by Flewelling and Hubbell (1985). The membrane-impermeable probe *N,N,N*-trimethyl-*N*-tempoylammonium iodide was synthesized by dissolving 4-amino-2,2,6,6-tetramethylpiperidinyl-1-oxy (0.50 g, ~2.9 mmol) into an excess volume (10 mL) of methyl iodide with the addition of triethylamine (0.6 g, 6.0 mmol). The mixture was refluxed for approximately 16 h, and the product was recrystallized from a mixture of acetone and methanol. The product gave a negative reaction with ninhydrin but produced a positive reaction with Dragendorff's reagent (Stahl, 1969).

Phospholipids and Vesicle Preparation. Egg phosphatidylcholine (egg PC) was prepared as described previously (Singleton et al., 1965) and was stored in chloroform at −20 °C under an argon atmosphere. All other phospholipids were obtained from Avanti Biochemicals (Birmingham, AL). Small sonicated vesicles were prepared as previously described (Castle & Hubbell, 1976), and vesicle sizes, determined by negative-stain electron microscopy, had average diameters ranging from approximately 300 to 500 Å. Large unilamellar vesicles were prepared by reverse-phase evaporation, ether injection, and detergent dialysis, followed by Millipore filtration according to published procedures (Szoka & Papahadjopoulos, 1980; Deamer, 1978; Mimms et al., 1981). Vesicles prepared by ether injection contained 10 mol % egg phosphatidic acid. Following preparation, the vesicle lipids were tested for oxidation by extraction and measurement of the 232/215-nm absorbance ratio as previously described (Bangham et al., 1974). All pH gradients were established by diluting vesicle suspensions into the appropriate buffer or by adding small amounts of base to the suspension. In each case, gradients were established so that $[H^+]_{in}[H^+]_{out} = 10^{-14}$. Vesicle suspensions contained 100 mM MES and/or MOPS buffers with 125 mM Na_2SO_4.

The lipid concentration of the vesicle suspensions was determined by phosphate analysis with a modification of the procedure of Bartlett (1959). For small sonicated vesicles, this concentration and the vessicle size were used to determine the ratio of external/internal aqueous volumes and the volumes of surface binding domains, V_o/V_i and V_{mo}/V_{mi}, respectively (Cafiso & Hubbell, 1978a). For large unilamellar vesicles, the volume ratio V_o/V_i was determined by adding small quantities (usually 0.2 mM) of the impermeant spin probe *N,N,N*-trimethyl-*N*-tempoylammonium iodide to the lipid–solvent mixture prior to vesicle formation. The fraction of the free signal intensity that could be broadened by the addition of potassium ferricyanide to the final vesicle suspension [usually 30 mM $K_3Fe(CN)_6$ was added] provided a measure of this aqueous volume ratio. All EPR spectra were recorded on a modified Varian V-4500 series spectrometer fitted with a rapid-mixing device.

Estimation of the Transmembrane Potential Δψ and pH Gradient ΔpH. Spin-labeled amphiphiles were used to determine both Δψ and ΔpH from measurements of their phase partitioning in vesicle systems as previously described (Cafiso & Hubbell, 1978a,b). Labels I and II were used to determine Δψ. The secondary alkyl amine label III was used to estimate

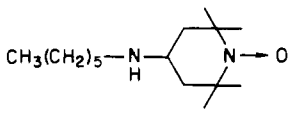

III

ΔpH. In all cases, the phase partitioning was determined by calibrating the intensity of the high-field nitroxide resonance ($m_I = -1$) in nanomoles of aqueous spin label.

Results

Estimation of H^+/OH^- Permeability in Large and Small Unilamellar Vesicles. When pH gradients are established across phospholipid vesicles, time-dependent changes in transmembrane potential occur until an electrochemical equilibrium is established for protons across the vesicle membrane. This potential change was shown to be due to an electrogenic transmembrane current of H^+ and/or OH^- ions across the phospholipid vesicle (Cafiso & Hubbell, 1983). Shown in panels A and B of Figure 1 are voltage-time curves for the development of a transmembrane potential following the establishment of a pH gradient in small sonicated vesicles and reverse-phase evaporation vesicles, respectively. Small amounts of Ph_4B^- (usually 1 μM or less) are added to these vesicle suspensions and ensure that the phosphonium transmembrane movement is not rate limiting (Cafiso & Hubbell, 1983). This level of Ph_4B^- has no effect upon the measured H^+/OH^- current. The equilibrium transmembrane voltages that were established (as measured by probe I or II are those predicted by an H^+ electrochemical equilibrium. Thus, our empirically determined values for V_o/V_i and V_{mo}/V_{mi} were consistent with the equilibrium voltages expected from an H^+ electrochemical equilibrium.

To estimate membrane permeabilities from the data shown in Figure 1, we will not distinguish between H^+ and OH^- flow and will calculate a net permeability, P_{net}, where

$$P_{net} = P_{H^+} + P_{OH^-} \quad (1)$$

This allows us to make a direct comparison with previous work

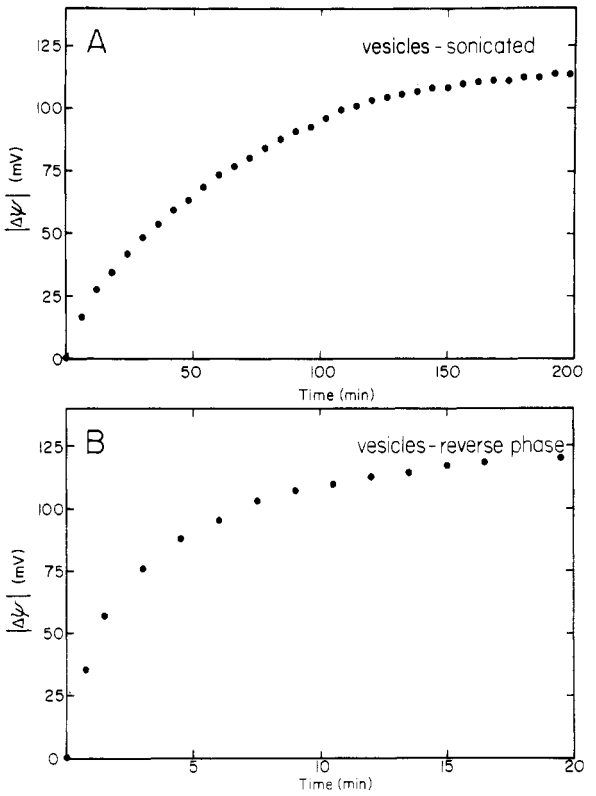

FIGURE 1: Time–voltage curves following the establishment of a pH gradient in (A) small sonicated vesicles of egg PC, ΔpH 2.1, and (b) reverse-phase evaporation vesicles formed from egg PC, ΔpH = 2.0. The measured equilibrium voltages are −121 and −119 mV for A and B, respectively. The points in the time–voltage curves are obtained from the time dependence of the high-field nitroxide resonance amplitude. From this amplitude, the phase partitioning of the hydrophobic paramagnetic phosphonium I and the transmembrane potential are calculated as described previously, see text.

[see, for example, Nichols & Deamer (1980) and Cafiso & Hubbell (1983)]. With experimental conditions arranged so that $[H^+]_{in}[H^+]_{out} = 10^{-14}$, the net proton permeability was calculated from the initial proton current (i_0), when $\Delta\psi = 0$, according to

$$i_0 = (\partial\psi/\partial t)_{\psi=0}c = FP_{net}([H^+]_{in} - [H^+]_{out}) \qquad (2)$$

where c is the specific membrane capacitance, F is the faraday constant, and $(\partial\psi/\partial t)_{\psi=0}$ is the initial slope of the voltage–time curves (Figure 1). At ΔpH = 2.0, the permeabilities for small sonicated vesicles and large vesicles prepared by reverse phase evaporation and by ether injection were 5.9 (±3) × 10^{-7}, 3.4 (±2) × 10^{-6}, and 2.6 × 10^{-6} cm/s, respectively. Vesicles prepared by detergent dialysis from octyl glucoside had a P_{net} of 8.6 (±1) × 10^{-6} cm/s (at a ΔpH of 1.0). Thus, small sonicated vesicles yielded the lowest net proton permeabilities by 5–10-fold compared to large unilamellar vesicles made by either reverse-phase evaporation, ether injection, or detergent dialysis.[2] When small sonicated vesicles were formed from lipids extracted from large vesicles, H^+/OH^- permeabilities of the sonicated vesicles were unchanged.

[2] The H^+/OH^- permeabilities determined here assume a constant membrane capacitance of 0.9 × 10^{-6} F/cm²; hence, differences in the vesicle capacitance as a function of vesicle size would alter the estimated H^+/OH^- permeabilities. It is unlikely, however, that differences in vesicle capacitance account for the differences in permeability seen here. As demonstrated previously, the value of 0.9 × 10^{-6} F/cm² obtained for planar systems (Montal & Mueller, 1972) works well in predicting equilibrium values of $\Delta\psi$ from the numbers of H^+/OH^- ions that move in small sonicated vesicle systems (Cafiso & Hubbell, 1983). For small vesicles, the membrane surface area used in determining the total capacitance is the mean geometric surface area $4\pi r_o r_i$, where r_o and r_i are the external and internal vesicle radii, respectively.

Table I: Effect of Lipid Composition upon H^+/OH^- Permeability[a]

lipid	no. of double bonds	permeability (cm/s)
POPC	1.0	7.0 × 10^{-7}
OPPC	1.0	2.0 × 10^{-7}
DOPC	2.0	6.0 × 10^{-6}
DLPC	4.0	8.0 × 10^{-6}
PAPC	4.0	5.6 × 10^{-6}
DAPC	8.0	1.8 × 10^{-5}

[a] All pH gradients were ΔpH = 1 with pH_{in} 6.5 and pH_{out} 7.5.

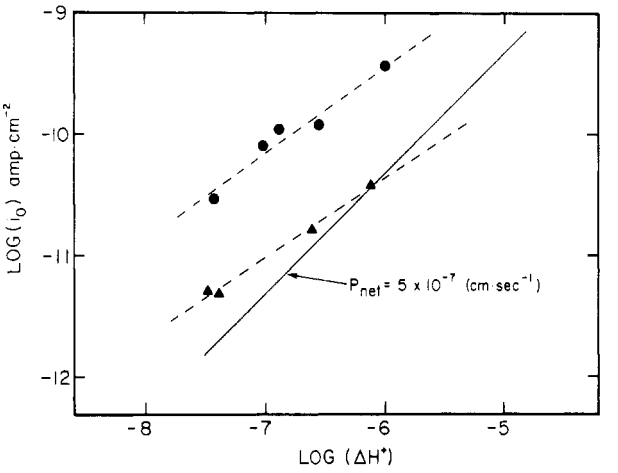

FIGURE 2: A log plot of the i vs. ΔH^+ behavior for SUVs (▲) and LUVs (●) (prepared by reverse-phase evaporation). In all cases, $[H^+]_{in}[H^+]_{out} = 10^{-14}$. Also shown is the expected behavior for a simple H^+ diffusion mechanism with a permeability of 5 × 10^{-7} (—), calculated with eq 2. The nonideal behavior of the H^+/OH^- current renders the phenomenological membrane permeability dependent upon ΔpH.

The composition of the phosphatidylcholines (PCs) used in these measurements had a significant effect upon P_{net}. For egg PC, a 5-fold variation in P_{net} was detected depending upon whether the PC was pooled from early or late fractions from the aluminum oxide column used during purification [see the procedure of Singleton et al. (1959)]. These PCs vary by small amounts in their composition of polyunsaturated fatty acids. An "early" fraction typically contained 2–3 times the levels of 20:4, 22:4, 22:5, and 22:6 fatty acids compared to "late" column fractions. Permeabilities for vesicles formed from several well-defined lipids are shown in Table I. Generally, lipids with higher levels of unsaturation exhibited higher net proton permeabilities, although the position of the double bonds also appeared to be important. Palmitoyloleoylphosphatidylcholine (POPC) differed significantly in its proton permeability depending upon whether oleic acid was in the first or second acyl position.

Dependence of the Proton Current and Apparent Permeability upon ΔpH. As previously shown, the net proton current is surprisingly insensitive to the magnitude of the hydrogen ion gradient ΔH^+ (Nichols & Deamer, 1980; Cafiso & Hubbell, 1983; Gutknecht, 1984). Hence, at a fixed value of the pH gradient, ΔpH, the estimated proton or hydroxyl permeability was highly dependent upon the value of ΔH^+ chosen (i.e., the pH at which the H^+/OH^- current was measured). The dependence of the net proton permeability upon ΔpH, when the experiment is performed about pH 7, also has a behavior that is not consistent with a simple diffusion mechanism. Shown in Figure 2 is a log plot of the net proton current vs. the H^+ gradient, ΔH^+, for both sonicated and reverse-phase vesicles where $[H^+]_{in}[H^+]_{out} = 10^{-14}$. In addition,

Table II: Dependence of P_{net} upon ΔpH[a]

ΔpH	j_0 (pC s^{-1} cm^{-2})	P_{net} (cm/s)
	SUVs	
1.8	37	4.9×10^{-7}
0.9	16	6.7×10^{-7}
0.14	4.9	2.3×10^{-6}
	LUVs	
2.0	360	3.8×10^{-6}
1.0	120	4.5×10^{-6}
0.4	80	1.0×10^{-5}

[a] Vesicles were all formed from the same sample of egg PC. In each case $[H^+]_{in}[H^+]_{out} = 10^{-14}$, and P_{net} was calculated with eq 2.

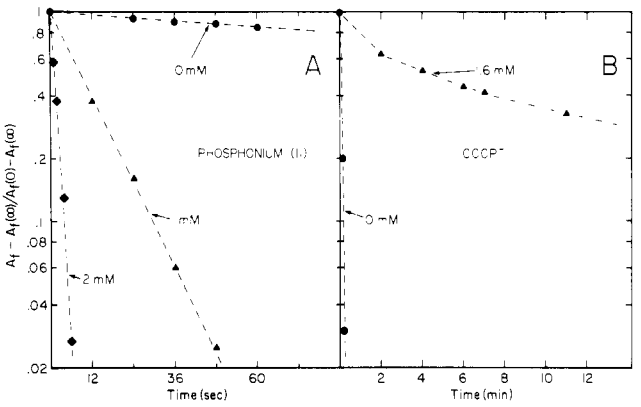

FIGURE 3: Effect of added phloretin upon the transmembrane migration of two charged species in sonicated egg PC vesicles is shown. In (A), the points represent the fractional change in the high-field nitroxide resonance ($m_I = -1$) of the phosphonium II following mixing with vesicles with (▲, ♦) and without (●) phloretin. This first-order decay represents the transmembrane migration of II. The fractional change is represented as $[A_f - A_f(\infty)]/[A_f(0) - A_f(\infty)]$, where A_f, $A_f(0)$, and $A_f(\infty)$ are the free signal intensities at any time t, $t = 0$, and equilibrium, respectively. In (B), the rate of decay of a weakly buffered pH gradient (10 mM MES buffer, pH 6.5) in the presence of 10 μM CCCP is followed with the alkylamine nitroxide (III). The points represent the fractional increase in the high-field resonance of III in the presence (▲) and absence (●) of phloretin. In the present case, the rate of decay in ΔpH is limited by the transmembrane diffusion of the CCCP anion. The nonexponential behavior of this curve is due, in part, to a titration of the buffer on the vesicle interior.

the predicted i vs. ΔH^+ behavior based upon eq 2 with a P_{net} of 5×10^{-7} cm/s is plotted. Because the slopes of the experimental curves are less than the curve predicted by eq 2, the estimated values of P_{net} are dependent upon ΔpH and *increase* as ΔpH decreases. A few of these apparent values of P_{net} were calculated from the points in Figure 2 and are listed in Table II.

Dipole Potential Changes and Proton Currents in Vesicles. To determine the proportion of the proton current that is due to positive vs. negative charge carriers, we altered the membrane dipole potential of small sonicated phospholipid vesicles by the addition of phloretin. Changes in the dipole potential were confirmed and estimated in these samples by examining the movement of known charge carriers. We measured the rate of movement of a positively charged phosphonium ion and the CCCP anion. The transmembrane movement of the phosphonium is easily measured by monitoring the high-field resonance of the phosphonium following rapid mixing with a vesicle suspension (Cafiso & Hubbell, 1982). Shown in Figure 3A is a recording of this resonance line following mixing in the presence and absence of phloretin. As expected, phloretin dramatically enhances the transmembrane migration rate of the phosphonium. The movement of the CCCP anion was monitored by measuring the decay in a pH gradient under weakly buffered conditions in the presence of CCCP. The

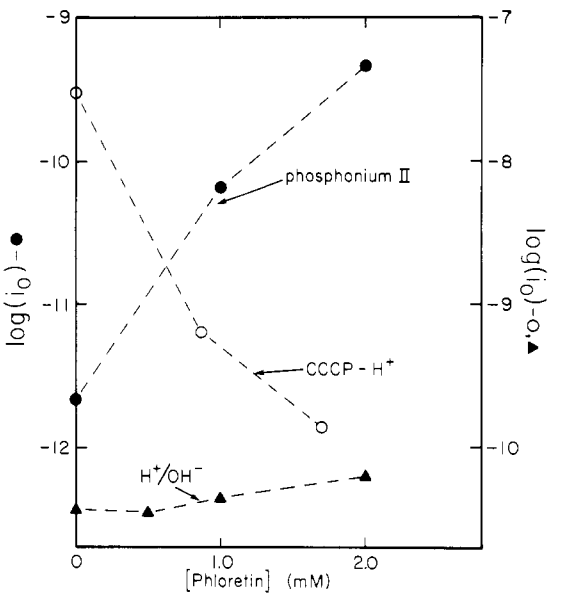

FIGURE 4: Plot of the effect of added phloretin upon the magnitudes of the phosphonium current (●), the H^+/OH current (▲), and the CCCP-induced proton current (○); all currents are given in units of A cm^{-2}. The egg PC vesicle suspension was at a concentration of 26 mM. The initial phosphonium current (i_0) was estimated as described previously (Cafiso & Hubbell, 1982). The initial CCCP-induced proton current was measured with label III in the presence of 10 μM CCCP with a 10 mM MES buffer solution in the vesicle interior (pH 6.5). The current was estimated from the initial change in ΔpH with a buffer capacity of 5×10^{-3} M pH^{-1} (Cafiso & Hubbell, 1983). Note that the H^+/OH^- and CCCP proton currents are plotted on a different scale than the phosphonium current.

secondary alkylamine nitroxide (III) was used to follow this gradient. Under these conditions, the proton current is dominated by the carrier and is expected to be rate limited by the transmembrane migration of the CCCP anion (McLaughlin & Dilger, 1980). The record of this ΔpH decay, shown in Figure 3b, clearly indicates that this expectation is met, since phloretin dramatically slows the ΔpH decay due to CCCP. The change in the high-field resonance of III is not linear on this semilog plot due to the titration of the vesicle internal buffer.

In these experiments, the vesicles are preequilibrated with 0.5–2.0 mM phloretin, which we assume distributes across the vesicle bilayer. The lack of a transmembrane potential difference between the bulk aqueous phases shortly after adding 1 mM phloretin (ca. within 1 min) argues that this assumption is correct. We have also examined the movement of phloretin directly. At the concentrations of lipid used in these experiments, 26 mM lipid, with 1 mM phloretin, a direct assay of the aqueous phloretin indicates that only 0.5% remains in the aqueous phase. Both the protonated and unprotonated forms of phloretin can be monitored spectrophotometrically by their absorbances at 284 and 320 nm, respectively. Membrane-associated phloretin remains in a protonated (uncharged) state down to at least a pH of 8 (the solution pK of phloretin is 7.3). The transmembrane migration of phloretin was followed by measuring its deprotonation in vesicles having a basic interior (pH 10). Within ca. 1 min, phloretin comes to a transmembrane equilibrium across the small sonicated vesicle systems used here.

From the data in Figure 3, the shift in dipole potential can be readily estimated with a simple Eyring analysis. We assume that phloretin modifies a central energy barrier to ion transport where the rate constants for transport with and without phloretin are k' and k, respectively. In this case, $\Delta\phi_d$ =

(RT/zF) ln (k/k'), where $\Delta\phi_d$ is the dipole potential change and z, R, T, and F have the usual meanings. Shown in Figure 4 are the currents for the phosphonium ion II, H^+/OH^- movement, and the CCCP-induced H^+ movement at several concentrations of phloretin. With 1 mM phloretin added, a dipole potential change of ~90 mV is produced as estimated from the rates of movement of both positive and negative carriers. Under these conditions, little change in the H^+/OH^- current (P_{net}) can be detected. Phloretin at the concentration and pHs used here does not act as a protonophore.[3]

Comparison of H^+/OH^- vs. D^+/OD^- Currents. The recent interest in proton wires as a mechanism to account for H^+/OH^- flow in membranes [see Nichols & Deamer (1980)] lead us to examine the deuterium isotope effect for the proton/hydroxide current (see discussion). For one set of identical experimental conditions in reverse-phase vesicles, where one buffer contained a minimum of 99% D_2O, we obtain permeabilities of 4.6 (±1.5) × 10^{-6} and 2.3 (±1) × 10^{-6} cm/s, respectively, for H_2O- and D_2O-containing buffers.

Discussion

Variability in the H^+/OH^- Flux. A wide range in the reported literature values for proton permeation in bilayers is found, even in cases where the experimental conditions are expected to yield directly comparable results. As we demonstrated previously, factors such as lipid oxidation and the removal of solvents from lipid preparations prior to sonication can have dramatic effects upon the apparent protonic current. As shown above, a number of other experimental factors have significant effects upon the estimated value of P_{net}. Small sonicated vesicles exhibit proton permeabilities that are approximately 5–10-fold lower than large unilamellar vesicles. This does not appear to result from an alteration (e.g., oxidation) of the membrane lipid in LUVs since lipids extracted from these vesicles can be used to form SUVs with a "normal" H^+/OH^- permeability. The addition of small quantities of diethyl ether that might be expected to be present in these LUV preparations has a relatively small effect upon P_{net}; thus, the difference in proton permeability appears to reflect a more fundamental structural difference between these vesicle types.

The effect of unsaturation (see Table I) is certainly another potential source of the discrepancy among the literature values for P_{net}. Fivefold differences among different fractions of egg PC are not unreasonable. Changes in P_{net} with unsaturation generally follow the changes in membrane dielectric that are expected with additional double bonds. The changes in P_{net} with unsaturation rise more rapidly than can be accounted for by calculating shifts in the average dielectric of the membrane (assuming an increase in relative dielectric constant of 0.25 per double bond). Thus, if the effects of double bonds are due to electrostatic energies, they must be discrete and local. The position of the double bonds as shown above is also important. At present, we do not understand these effects, but they do not appear to be the result of lipid purity or oxidation.

The value of the pH gradient chosen has a large effect upon the estimated P_{net}. This is not too surprising considering the unusual dependence of P_{net} upon the H^+ gradient that has been observed and is again a strong indication that H^+/OH^- permeability is not the result of a simple diffusion process. As

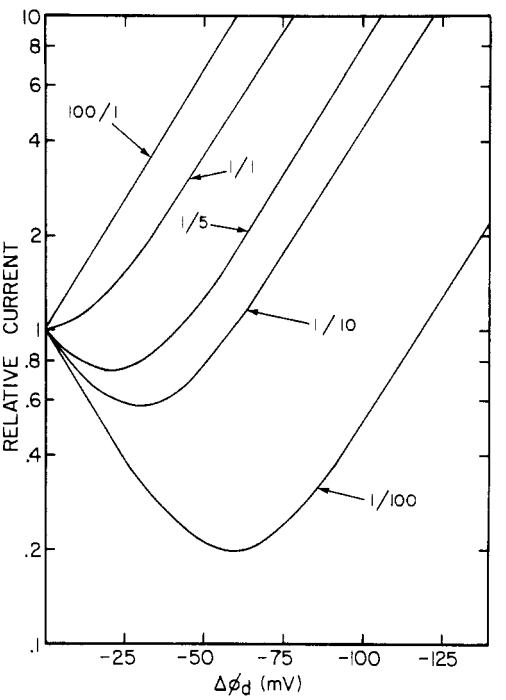

FIGURE 5: Plot of the relative current vs. the change in dipole field $\Delta\phi_d$ for several currents that are composed of both positive and negative components. The ratio that is given is the ratio of positive/negative charge contributing to the total membrane current. The plot was calculated simply from an Eyring rate theory, assuming that $\Delta\phi_d$ modifies the magnitude of an energy barrier to ion transport in the membrane interior.

a result, direct comparisons between measurements made in the presence of large pH gradients [see Cafiso & Hubbell (1983)] and those where ΔpH values are small (for example, the pH electrode measurements of Nichols and Deamer) cannot be made. At least a 10-fold difference in P_{net} between these two measurements can be accounted for simply by the nonideal i vs. ΔpH behavior. The i vs. ΔpH behavior obviously may provide insight into the mechanisms of H^+/OH^- permeation through bilayers, but we will not attempt an analysis of this behavior here.

Measurements made with the techniques described here yield permeabilities that are 3 orders of magnitude lower than the value reported by Nichols and Deamer (1980). When vesicle size and the experimental values of ΔpH are taken into account, there is approximately an order of magnitude discrepancy, a difference that might easily be due to vesicle lipid composition. Thus, among measurements that have been made to determine P_{net} for proton fluxes, the wide range of some experimental values that have been reported can be readily accounted for. Implicit in the calculations of membrane permeability for H^+/OH^- flow (e.g., eq 2) are simple diffusion models. Since such models do not adequately describe H^+/OH^- currents in vesicles, the wide range in experimental permeabilities is not surprising. It should be noted that although the currents generated by proton gradients exceed that for other monovalent ions in pure lipid systems, these currents are expected to be small compared to those generated by active transport systems.

Electrical Characteristics of the H^+/OH^- Current. The possibility that negative as well as positive currents might contribute to the proton current has not been examined and could provide insight into the carrier mechanism(s). The experiments performed here, modifying the dipole field of model membrane systems, were designed to determine the sign of the charge carrier. In Figure 5 is shown the expected

[3] At much higher concentrations of phloretin (above 4 mM), H^+/OH^- currents are significantly enhanced in egg PC vesicles. This phloretin effect is more pronounced at higher pHs (near phloretin's pK) and is presumably the result of phloretin's limited activity as a proton carrier. In its charged form, phloretin apparently does not modify the dipole potential (Andersen et al., 1976).

behavior of a membrane current when the dipole field is modified. The series of curves represent total currents that are composed of different proportions of positive and negative current (the positive/negative current ratio is given). The response in each case to changes in the dipole field is unique. As shown above, dipole fields can be modified in vesicle systems by the addition of phloretin. The carriers and charged species we have examined show the expected behavior in vesicle systems. Surprisingly, the proton current shows little dependence upon the membrane dipole field (Figure 3). Hence, alterations of electrostatic energy barriers within the membrane hydrocarbon (i.e., lying deeper than the region where the dipole field is modified) have little effect upon the protonic current. This result argues against small amounts of contaminating or intrinsic carriers as a mechanism for H^+/OH^- permeation, since such carriers should be sensitive to the dipole field.

As observed previously (Cafiso & Hubbell, 1983), we measure highly linear current–voltage curves (up to at least 80 mV) when the H^+/OH^- current is plotted vs. $\Delta\psi - \Delta\psi_{eqm}$ [$\Delta\psi_{eqm} = (-RT/zF) \ln([H^+]_{in}/[H^+]_{out})$]. If the transport of H^+/OH^- ions is diffusion-limited by an electrostatic energy barrier in the membrane interior, we expect the following current–voltage behavior, assuming a simple trapezoidal barrier:

$$i = zFP_{net}\{[H^+]_{in} \exp[(1 - n)\phi] - [H^+]_{out} \exp(-n\phi)\}$$

where n determines the thickness of the trapezoidal barrier and ϕ is the reduced potential $zF\Delta\psi/RT$ [see Hall et al. (1974)]. Plots of the current i vs. $\Delta\psi - \Delta\psi_{eqm}$ yield hyperbolic curves. For both broad and narrow barriers, this behavior is seen; linear i–v curves such as those obtained experimentally cannot be obtained with this barrier shape. This observation is consistent with the lack of a dipole potential effect upon H^+/OH^- conduction, since it strongly suggests that a simple diffusion of ions over a large central electrostatic energy barrier is not the rate-limiting step in H^+/OH^- conduction.

Hydrogen-bonded water chains have been proposed to account for H^+/OH^- conduction in lipid vesicles (Nichols & Deamer, 1980). This model has received considerable attention and may account for several features of the H^+/OH^- current. If this model is correct, the H^+/OH^- conductivity might be expected to vary with the number of chains present. We attempted to test this possibility by measuring D^+/OD^- conductivities. Water that has been placed into the hydrocarbon as a chain will have approximately two less hydrogen bonds compared to bulk water. Since deuterium bonds are generally stronger than hydrogen bonds, the energy of a D_2O chain is expected to be greater than that of a H_2O chain. Hence, we expected fewer chains to be formed in D_2O. In our measurement, D^+/OD^- currents were virtually identical with H^+/OH^- currents (within experimental error).

Unfortunately, predicting the extent of an isotope effect here is difficult. Some estimates of D vs. H bond energies suggest this isotope effect should be large. For example, in isomeric dimers, $H_2O\cdots DOH$ is favored over $H_2O\cdots HOD$, and $HF\cdots DF$ is favored over $DF\cdots HF$. Estimates of the energy differences for these species are on the order of 2 kJ/mol, in favor of the D bond. However, in other model systems the energy differences can be small, and H-bonded species are even sometimes slightly favored (Buckingham & Fan-Chen, 1981). Thus, the H vs. D bond energy is highly structure dependent and estimates of D_2O vs. H_2O chain energy differences may not be possible from energy differences in these simple model systems. At the present time, it is difficult to rule out the water chain mechanism on the basis of the lack of an isotope effect seen here.

Other published data argue against the role of H-bonded chains; recent FTIR data indicate that water remains as a monomer when dissolved into hydrocarbon (Conrad & Strauss, 1985). However, because the state and behavior of water in bilayers (as opposed to bulk hydrocarbon systems) is not well understood, definitive conclusions are again difficult to make. There may also be membrane-associated water, not necessarily in a chain, that can account for the behavior and magnitude of this H^+/OH^- current.

In conclusion, a number of experimental features including vesicle size, lipid unsaturation, and the magnitude of the pH gradients chosen affect the values of the phenomenological permeability for H^+/OH^- ions that are measured in bilayers. We believe that much, if not all, of the discrepancy among the reported values can be accounted for by these factors. This anomolously high permeability does not appear to be rate limited by membrane electrostatic barriers as the currents are insensitive to changes in membrane dipole field. This result argues against the presence of small amounts of contaminants acting as H^+/OH^- carriers. There is also little difference between the magnitude of D^+/OD^- vs. H^+/OH^- currents in vesicle systems.

Acknowledgments

We thank Drs. Wayne L. Hubbell, Lester W. Andrews, Stuart G. McLaughlin, and John F. Nagle for helpful discussions during the course of this work.

Registry No. I, 65643-91-6; II, 100791-13-7; III, 67972-72-9; CCCP, 555-60-2; POPC, 6753-55-5; OPPC, 17118-56-8; DOPC, 10015-85-7; DLPC, 6542-05-8; PAPC, 6931-56-2; DAPC, 17688-29-8; H^+, 12586-59-3; OH^-, 14280-30-9; D^+, 14464-47-2; OD^-, 17693-79-7; *N,N,N*-trimethyl-*N*-tempoylammonium iodide, 64525-01-5; 4-amino-2,2,6,6-tetramethylpiperidinyl-1-oxy, 14691-88-4; methyl iodide, 74-88-4; phloretin, 60-82-2.

References

Andersen, O. F., Finkelstein, A., Katz, I., & Cass, A. (1976) *J. Gen. Physiol. 67*, 749–771.

Bantham, A. D., Hill, M. W., & Miller, N. G. (1974) *Methods Membr. Biol. 1*, 1–68.

Bartlett, G. R. (1959) *J. Biol. Chem. 243*, 466–468.

Biegel, C. M., & Gould, J. M. (1981) *Biochemistry 20*, 3474–3479.

Buckingham, A. D., & Fan-Chen, L. (1981) *Int. Rev. Phys. Chem. 1*, 253–269.

Cafiso, D. S., & Hubbell, W. L. (1978a) *Biochemistry 17*, 187–195.

Cafiso, D. S., & Hubbell, W. L. (1978b) *Biochemistry 17*, 3871–3877.

Cafiso, D. S., & Hubbell, W. L. (1982) *Biophys. J. 39*, 263–272.

Cafiso, D. S., & Hubbell, W. L. (1983) *Biophys. J. 44*, 49–57.

Castle, J. D., & Hubbell, W. L. (1976) *Biochemistry 15*, 4818–4831.

Clement, N. R., & Gould, J. M. (1981) *Biochemistry 20*, 1534–1538.

Conrad, M. P., & Strauss, H. L. (1985) *Biophys. J. 48*, 117–124.

Deamer, D. W. (1978) *Ann. N.Y. Acad. Sci. 308*, 250–258.

Deamer, D. W., & Nichols, J. W. (1983) *Proc. Natl. Acad. Sci. U.S.A. 80*, 165–168.

Dutta-Choudhury, M. K., Mlljevic, N., & Van Hook, W. A. (1982) *J. Phys. Chem. 86*, 1711–1721.

Elamrani, K., & Blume, A. (1983) *Biochim. Biophys. Acta 727*, 22–30.

Flewelling, R., & Hubbell, W. L. (1986) *Biophys. J. 49*, 531–540.
Gutknecht, J. (1984) *J. Membr. Biol. 82*, 105–112.
Gutknecht, J., & Walker, A. (1981) *Biochim. Biophys. Acta 641*, 183–188.
Hauser, H., Phillips, M. C., & Stubbs, M. (1972) *Nature (London) 239*, 342–344.
Johnson, S. M., & Banghan, A. D. (1969) *Biochim. Biophys. Acta 193*, 82–91.
Krishnamoorthy, G., & Hinkle, P. C. (1984) *Biochemistry 23*, 1640–1645.
McLaughlin, S., & Dilger, J. (1980) *Physiol. Rev. 60*, 825–863.
Mimms, L. T., Zampighi, Y., Nozaki, Y., Tanford, C., & Reynolds, J. A. (1981) *Biochemistry 20*, 833–840.
Montal, M., & Mueller, P. (1972) *Proc. Natl. Acad. Sci. U.S.A. 69*, 3561–3566.
Nichols, J. W., & Deamer, D. W. (1980) *Proc. Natl. Acad. Sci. U.S.A. 77*, 2038–2042.
Nichols, J. W., Hill, M. W., Bangham, A. D., & Deamer, D. W. (1980) *Biochim. Biophys. Acta 596*, 393–403.
Nozaki, Y., & Tanford, C. (1981) *Proc. Natl. Acad. Sci. U.S.A. 78*, 4324–4328.
Pike, M. M., Simon, S. S., Balschi, J. A., & Springer, C. S., Jr. (1982) *Proc. Natl. Acad. Sci. U.S.A. 79*, 810–814.
Rossignol, M., Thomas, P., & Grignon, C. (1982) *Biochim. Biophys. Acta 684*, 194–199.
Singleton, W. S., Gray, M. S., Brown, M. L., & White, J. L. (1965) *J. Am. Oil Chem Soc. 42*, 53–57.
Stahl, E. (1969) *Thin Layer Chromatography*, 2nd ed., Wiley, New York.
Szoka, F., & Papahajopoulous, D. (1980) *Annu. Rev. Biophys. Bioeng. 9*, 467–508.

Iron-Depleted Reaction Centers from *Rhodopseudomonas sphaeroides* R-26.1: Characterization and Reconstitution with Fe^{2+}, Mn^{2+}, Co^{2+}, Ni^{2+}, Cu^{2+}, and Zn^{2+} †

R. J. Debus,‡ G. Feher, and M. Y. Okamura*
Department of Physics, University of California at San Diego, La Jolla, California 92093
Received August 29, 1985

ABSTRACT: Reaction centers (RCs) from the photosynthetic bacterium *Rhodopseudomonas sphaeroides* R-26.1 were depleted of Fe by a simple procedure involving reversible dissociation of the H subunit. The resulting intact Fe-depleted RCs contained 0.1–0.2 Fe per RC as determined from atomic absorption and electron paramagnetic resonance (EPR) spectroscopy. Fe-depleted RCs that have no metal ion occupying the Fe site differed from native RCs in the following respects: (1) the rate of electron transfer from Q_A^- to Q_B exhibited nonexponential kinetics with the majority of RCs having a rate constant slower by only a factor of ~2, (2) the efficiency of light-induced charge separation ($DQ_A \rightarrow D^+Q_A^-$) produced by a saturating flash decreased to 63%, and (3) Q_A appeared readily reducible to Q_A^{2-}. Various divalent metal ions were subsequently incorporated into the Fe site. The electron transfer characteristics of Fe-depleted RCs reconstituted with Fe^{2+}, Mn^{2+}, Co^{2+}, Ni^{2+}, Cu^{2+}, and Zn^{2+} were essentially the same as those of native RCs. These results demonstrate that neither Fe^{2+} nor *any* divalent metal ion is required for rapid electron transfer from Q_A^- to Q_B. However, the presence of a metal ion in the Fe site is necessary to establish the characteristic, native, electron-transfer properties of Q_A. The lack of a dominant role of Fe^{2+} or other divalent metals in the observed rate of electron transfer from Q_A^- to Q_B suggests that a rate-limiting step (for example, a protonation event or a light-induced structural change) precedes electron transfer.

The photochemical events of photosynthesis take place in a membrane-spanning complex of pigment and protein called the reaction center (RC).[1] RCs from the purple non-sulfur bacterium *Rhodopseudomonas sphaeroides* R-26.1 are composed of three 30–35-kDa polypeptides (designated L, M, and H) plus the following cofactors: four bacteriochlorophylls (BChl), two bacteriopheophytins (BPh), two ubiquinones (Q-10), and one atom of high-spin Fe^{2+}. A dimer of BChl serves as primary electron donor (D), and the two ubiquinones, Q_A and Q_B, serve as primary and secondary electron acceptors, respectively. Between D and Q_A is an intermediate acceptor, I, believed to be monomeric BPh interacting with BChl. Both Q_A and Q_B are magnetically coupled to the Fe^{2+} [for reviews, see Feher & Okamura (1978, 1984), Okamura et al. (1982a,b), Parson & Ke (1982), Wraight (1982) and Crofts & Wraight (1983)].

† Supported by grants from the National Institutes of Health (GM-13191) and the National Science Foundation (82-CRCR-1-1043). R.J.D. was the recipient of a U.S. Public Health Service predoctoral traineeship (5T32 AM-07233).
‡ Work performed in partial fulfillment for the Ph.D. degree (chemistry). Present address: M.S.U.–D.O.E. Plant Research Laboratory, Michigan State University, East Lansing, MI 48824.

[1] Abbreviations: RC(s), reaction center(s); Q-10, ubiquinone-50; Q-0, 2,3-dimethoxy-5-methyl-1,4-benzoquinone; cyt, cytochrome *c*; LDAO, lauryldimethylamine *N*-oxide; DEAE, diethylaminoethyl; Tris, tris(hydroxymethyl)aminomethane; PIPES, piperazine-*N*,*N*′-bis(2-ethanesulfonic acid); EDTA, (ethylenedinitrilo)tetraacetic acid; EPR, electron paramagnetic resonance; ENDOR, electron nuclear double resonance; EXAFS, extended X-ray absorption fine structure; Da, dalton.

0006-2960/86/0425-2276$01.50/0